

Effects of Iodine Content in the Electrolyte on the Charge Transfer and Power Conversion Efficiency of Dye-Sensitized Solar Cells under Low Light Intensities

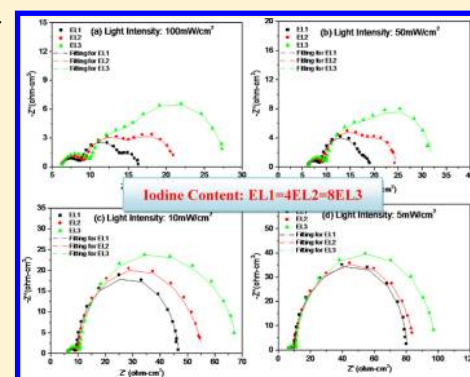
Jo-Lin Lan,[†] Tzu-Chien Wei,^{*,‡} Shien-Ping Feng,[§] Chi-Chao Wan,[‡] and Guozhong Cao^{*,†}

[†]Department of Materials Science and Engineering, University of Washington, Seattle, Washington, United States

[‡]Department of Chemical Engineering, National Tsing-Hua University, Hsin-Chu, Taiwan

[§]Department of Mechanical Engineering, The University of Hong Kong, Hong Kong

ABSTRACT: This paper presents a systematic investigation on the effects of iodine content in the electrolyte on electron recombination, charge, and ion transportation to the power conversion performance of dye-sensitized solar cells under lower light intensities. By analyzing the current–voltage behavior and electrochemical impedance spectroscopy results, the effects of iodine content on charge recombination, ion transportation, and light intensity are found to be the major factors. The power conversion efficiency of DSSC under low light intensity can be significantly improved when electrolyte composition is optimized, which results in an exclusive application for indoor use.



1. INTRODUCTION

Dye-sensitized solar cell (DSSC) has attracted much attention for its low material and process cost and relatively high conversion efficiency (>13%).^{1–6} A standard DSSC consists of a dye-sensitized nanocrystalline semiconductor film^{2,7,8} on transparent conductive oxide (TCO) glass as the photoanode, a cathode usually being a catalytic material for redox reaction, such as platinum,^{9–11} on TCO glass, and an iodide/tri-iodide redox couple in a proper medium as the electrolyte.¹² The DSSC working principal can be briefly described as follows:^{3,13} A dye molecule self-assembled on the surface of mesoporous TiO₂ photoanode absorbs a photon of the incident light, and the resulting excited electron on the lowest unoccupied molecular orbital (LUMO) is injected rapidly into the conduction band of the TiO₂ and subsequently diffuses to the TCO glass. Oxidized dye molecules are then reduced by I[−] in the electrolyte, and I[−] is oxidized to form I₃[−]. At the Pt electrode, the reverse reaction takes place to reduce I₃[−] back to I[−] to complete the entire cycle. Therefore, the total reaction involves only photon and electron with no physical material consumption. To obtain the high power conversion efficiency, the following aspects or parameters play important roles: the amount or fraction of photons captured and the amount or fraction of excited electrons transported out. The more photons are captured, the more electrons are generated and the generated electrons then need to be efficiently transported out to achieve a high power conversion efficiency.

To transport the electrons out with minimal loss, several interfaces could affect electron transfer including electron transfer from TiO₂ film to TCO glass, the TiO₂ film/dye/

electrolyte interface, and the cathode/electrolyte interface.^{14–16} To achieve high conversion efficiency, it is very important to determine the optimal conditions of these interfaces.¹⁷ Electrochemical impedance spectroscopy (EIS) is a powerful tool to interpret the kinetics of electrochemical interfaces and help us improve the performance of DSSC^{15,18,19} or monitor interface changes at aged conditions^{19–21} and optimize conditions for highly efficient cells.^{17,22}

In comparison with silicon-based solar cells, DSSC offers a great advantage for use indoors or under a low intensity of angled incident light as it retains nearly the same power conversion performance.⁴ However, little research was reported in the literature focusing on the fundamental understanding and technical know how of the relationships between power conversion efficiency, electron transfer, device structural parameters, and chemical compositions of the electrolyte. In this paper, we aim to understand the impacts of optimizing electrolyte composition under various lower intensity light illumination conditions. The relationship and possible mechanisms of the impact of iodine content on charge transfer, recombination, and power conversion efficiency at lower light intensity are discussed.

2. EXPERIMENTAL SECTION

2.1. Preparation of the PVP-Capped Pt Nanoclusters Counter Electrode.

A “two-step dip-coating” process^{10,23–25}

Received: October 5, 2012

Revised: November 5, 2012

Published: November 17, 2012

was utilized to prepare PVP-capped Pt nanoclusters counter electrode (PVP-Pt CE). FTO glass ($7 \Omega/\square$, 2.2 mm thick, Pilkington) was first immersed in 4% conditioner (ML371, OM Group) for 5 min at 60°C followed by activation with PVP-capped Pt nanoclusters for 5 min at 40°C . After each step, the FTO glass was rinsed with deionized water, dried in open air, and finally heated in a furnace at 350°C for 10 min. Since this is a dip-coating process in aqueous solution, this kind of counter electrode can be made in vast volume within hours.

2.2. Preparation of the Mesoporous TiO_2 Photoanode.

A trilayer photoanode containing a TiO_2 underlayer and a mesoporous and light scattering layer was prepared as follows: FTO glass ($10 \Omega/\square$, 3.1 mm thick, Nippon Sheet Glass) was cleaned in a supersonic bath for 5 min twice: the first bath contained 5% glass cleaner (PK-LCG545, Parker), and the second bath contained deionized water only. Afterward, it was immersed into 40 mM TiCl_4 aqueous solution at 70°C for 30 min and washed with water and ethanol; the purpose of this treatment was to form a thin and dense TiO_2 underlayer to restrain dark current;²⁶ then homemade nano- TiO_2 paste (particle size 20 nm) was screen-printed on pretreated FTO glass repeatedly until the film thickness reached $10 \mu\text{m}$. Finally, a $4 \mu\text{m}$ light scattering film (CCIC, PST400) was screen-printed on nano- TiO_2 film. The trilayer film was then sintered at 500°C for 30 min in a furnace. In order to enhance the electron diffusivity in mesoporous TiO_2 film, post-treatment was done by placing as-prepared film into 40 mM TiCl_4 solution at 70°C for 30 min again to form a necking layer.^{26,27} After being washed with water and ethanol, it was annealed again at 500°C for 30 min to complete the photoanode preparation. Dye impregnation was done by immersing the TiO_2 photoanode in a 0.4 mM N719 (D719, Everlight Chemical Industrial Corp.) ethanol solution at 40°C for 20 h. The effective area of the TiO_2 photoanode is 0.283 cm^2 .

2.3. Electrolyte Formulation.

Three kinds of electrolyte were developed to test the DSSC performance under various light intensities. Electrolyte 1 (EL1) consisted of 1 M 1,3-dimethylimidazolium iodide (DMII, Merck), 0.15 M iodine (I_2 , J. T. Baker), 0.1 M guanidine thiocyanate (GuSCN, Sigma-Aldrich), and 0.5 M 4-*tert*-butylpyridine (4-tBP, Aldrich) in 3-methoxypropionitrile (3-MPN, Acros). Electrolytes 2 (EL2) and 3 (EL3) had the same composition except that the concentration of tri-iodide, $[\text{I}_3^-]$, was 0.0375 (25% of the concentration in EL1) and 0.01875 M (12.5% of EL1 and 50% of EL3), respectively. All chemicals were purchased and used without further purification. Three electrolyte systems were injected into the sealed cells via predrilled holes on the counter electrode side, and injection holes were hot sealed by a piece of thin cover glass with a hot-melt film underneath as the adhesive. The gap between photoanode and cathode is $30 \mu\text{m}$.

2.4. Characterization.

EIS was measured by scanning the DSSC cell with a computer-controlled potentialstat (Autolab PGSTAT320N) from 100 kHz to 0.1 Hz with 10 mV amplitude at open-circuit conditions under various light intensities. The limiting current of each electrolyte was determined by measuring the linear sweep voltammogram (LSV) of a 2-compartment electrochemical cell (Pt micro-electrode ($\varphi = 20 \mu\text{m}$) as the reference electrode and a Pt sheet (4 cm^2) as the working electrode using an Autolab PGSTAT320N from -0.75 to 0.75 V with a 5 mV/s scan rate. Ultraviolet–visible spectroscopy (UV–vis) was measured by MFS-630 (Hong-Ming Technology Co., Ltd.) from 350 to

800 nm. The current–voltage (*IV*) curve of DSSC was measured with a computer-controlled digital source meter (Keithley 2400) under exposure of a standard solar simulator (YAMASHITA DENSO YSS-150A. AM1.5, ClassA). Light intensity was controlled by a neutral density filter (NDS0, ND10, NDS, Shibuya Optics).

3. RESULTS AND DISCUSSION

The standard EIS spectrum of a highly efficient DSSC (PCE > 8% with EL1 under 1 sun illumination) and the corresponding equivalent circuit model are shown in Figure 1. From EIS

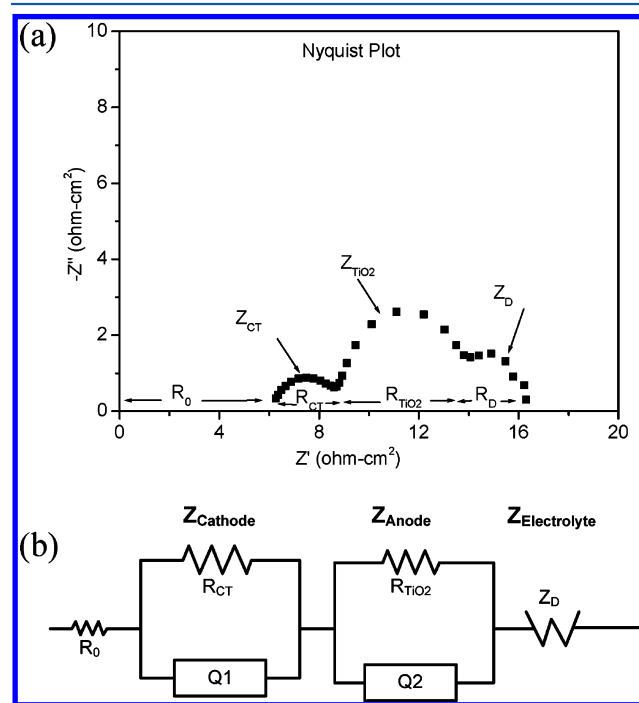


Figure 1. (a) Nyquist plot of DSSC with PCE > 8% at 1 sun and (b) its equivalent circuit model.

theory,^{14–16,19,28–30} each semicircle represents a charge transfer process at different interfaces and the semicircles in the frequency regions 10^3 – 10^5 , 1 – 10^3 , and lower than 1 Hz are attributed to impedance related to charge transfer through the counter electrode (R_{CT}), electron recombination on the interface of TiO_2 /dye/electrolyte (Z_{TiO_2}), and electrolyte diffusion (Z_D), respectively. In front of Z_{CT} , R_0 consists of the sheet resistance of the TCO glass, contact resistance, and wire resistance. Twelve DSSCs are investigated including 3 kinds of electrolytes (EL1, EL2, and EL3) and 4 levels of light intensities (100 , 50 , 10 , and 5 mW/cm^2). *IV* curves of these cells are plotted in Figure 2, and their corresponding parameters are listed in Table 1. Meanwhile, EIS of these cells are scanned, and the Nyquist plots including fitting curves are shown in Figure 3. By fitting curves of Nyquist plots, these impedance elements can be obtained and are summarized in Table 2.

As will become clear from this study, the influences of iodine content in the electrolyte on the power conversion process in DSSC are multifaceted and complex. To better present the experimental results and the relationship between power conversion efficiency (PCE) and iodine content or light intensity, the trends of V_{OC} , J_{SC} , Z_D , R_{CT} , FF, and PCE when

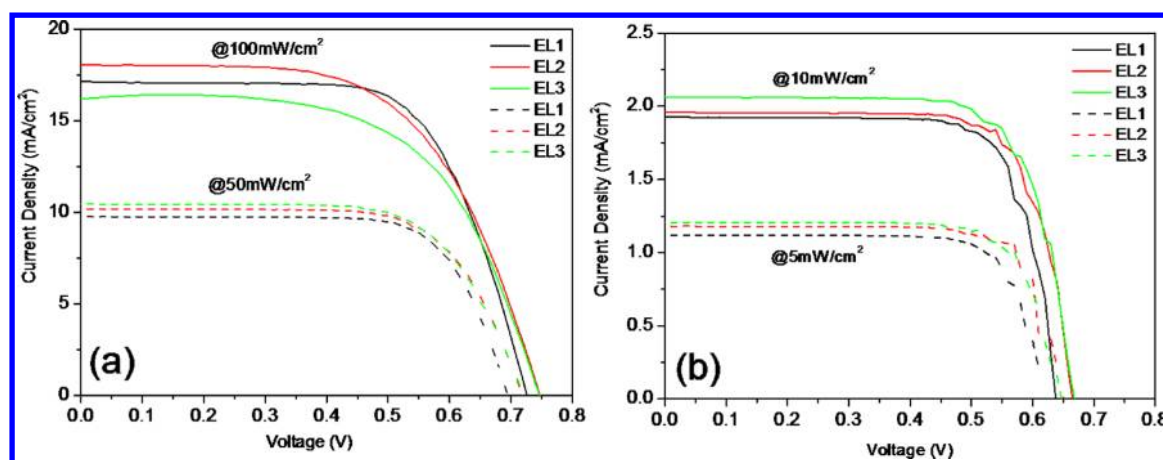


Figure 2. IV curves of DSSCs composed of various electrolytes under various conditions: (a) 100 and 50 mW/cm² and (b) 10 and 5 mW/cm².

Table 1. IV Parameters of DSSCs Composed of Various Electrolytes under Various Light Intensities

light intensities (mW/cm ²)	electrolyte formula	J_{SC} (mA/cm ²)	V_{OC} (V)	FF	PCE (%)
100	EL1	17.15	0.73	0.67	8.31
	EL2	18.07	0.75	0.59	8.02
	EL3	16.18	0.75	0.60	7.28
50	EL1	9.76	0.69	0.72	9.79
	EL2	10.19	0.72	0.69	10.08
	EL3	10.46	0.72	0.67	10.16
10	EL1	1.93	0.64	0.76	9.31
	EL2	1.96	0.67	0.76	9.93
	EL3	2.06	0.67	0.75	10.36
5	EL1	1.12	0.62	0.76	10.58
	EL2	1.18	0.65	0.78	11.99
	EL3	1.21	0.65	0.77	12.03

iodine content or light intensity varies are discussed first separately.

Influence of Iodine Content on the Open-Circuit Voltage, V_{OC} . V_{OC} of a DSSC can be described by the following equation²⁸

$$V_{OC} = \frac{kT}{q} \ln \left(\frac{\eta \Phi_0}{n_0 k_{et} [I_3^-]} \right) \quad (1)$$

where k is the Boltzmann constant, q is the magnitude of the electron charge, T is the absolute temperature, η is the quantum yield for photogenerated electrons, Φ_0 is the incident photon flux, n_0 is the electron density on the conduction band of the TiO₂ in the dark, k_{et} is the rate constant for recombination, and $[I_3^-]$ is the concentration of tri-iodide in solution. Tri-iodide is formed instantaneously when iodine is added in solution which contains iodide via the equation $I^- + I_2 \rightarrow I_3^-$. Apparently, from eq 1, V_{OC} increases as $[I_3^-]$ decreases; this is consistent to the IV parameters in Table 1. The relation between V_{OC} and $[I_3^-]$ can be further explained by EIS; the impedance of mesoporous TiO₂ film, Z_{TiO_2} , is described as³⁰

$$Z_{TiO_2} = \left(\frac{R_d R_r}{1 + i\omega/\omega_r} \right)^{1/2} \coth[(\omega_r/\omega_d)^{1/2} (1 + i\omega/\omega_r)^{1/2}] \quad (2)$$

where R_d and R_r are the electron transfer and electron recombination resistance and ω_d and ω_r are their corresponding

characteristic frequencies. For a highly efficient DSSC, R_d is usually too small to be identified by EIS and only R_r will appear on the spectrum.³⁰ In addition, R_d usually relates to the structure of the mesoporous nanocrystalline TiO₂ film and is not affected by electrolyte formulation. Therefore, it is reasonable to treat the change of R_{TiO_2} as the change of R_r only; R_r is generally acknowledged as the charge transfer resistance of the following reaction happening at the dye–TiO₂/electrolyte interface



R_{TiO_2} of EL1–EL3 under various light intensities as a function of V_{OC} is plotted in Figure 4. R_{TiO_2} increases from 4.86 to 5.48 ohm-cm² as $[I_3^-]$ decreases from 0.15 (EL1) to 0.01825 M (EL3) under 100 mW/cm² light illumination, suggesting the reaction of eq 3 is hindered because of less tri-iodide in the electrolyte, which is in a good agreement with the literature results.^{31,32} Similarly, R_{TiO_2} increases monotonically, though not necessarily linearly, with a reduced iodine concentration at lower light intensities. In addition, R_{TiO_2} increases rapidly with a reduced light intensity when the electrolyte with the same iodine concentration was used. Taking the EL1 system as example, R_{TiO_2} increased from 4.86 to 68.14 ohm-cm² when the light intensity decreased from 100 to 5 mW/cm². Such an increase in R_{TiO_2} would result in less electron recombination taking place at the interface of TiO₂/dye/electrolyte. This result can be also interpreted by eq 3 since fewer photoelectrons are generated at lower light conditions than stronger ones and therefore retard the recombination reaction. For the decrease in V_{oc} under lower light intensity, it can be explained that the Fermi level of TiO₂ decreases due to fewer photoelectrons being generated and injected.³³

Influence of Iodine Content on the Short-Circuit Current Density, J_{SC} . According to previous research,² J_{SC} of a DSSC should have a linear dependence on light intensity (at least to 100 mW/cm²). However, if we further consider the iodine content in the electrolyte of a DSSC, the linear relation of J_{SC} needs to be modified because of the deep brown color nature of the iodide/iodine redox couple system. Iodide/iodine redox is known to have absorption from 350 to 650 nm where it overlaps the photoresponse region of N719-based DSSC.

Figure 5 is the UV–vis spectrum of EL1–EL3. As shown in Figure 5, EL1 contains the most iodine and shows the deepest brown color, which means the incident light will be trapped more in the 350–650 nm region when compared to EL2 and

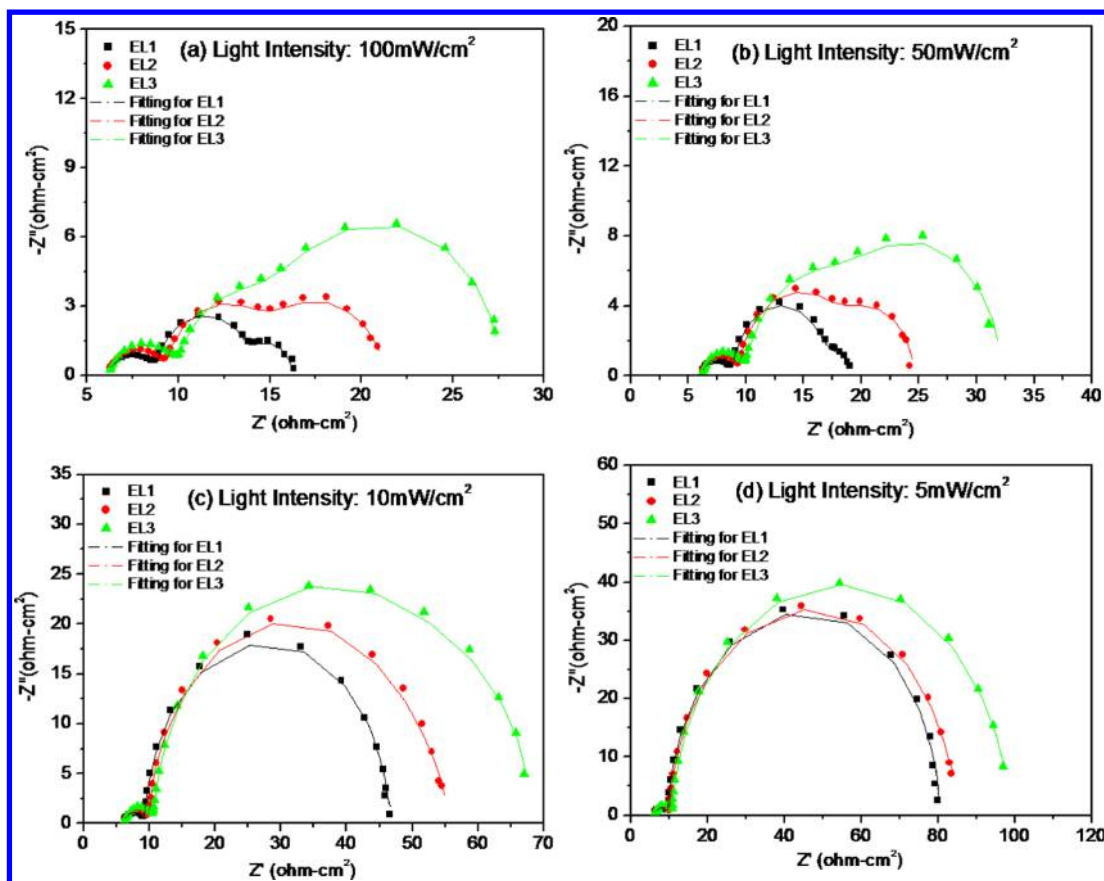


Figure 3. Nyquist plots and fitting curves of DSSCs with various electrolytes under various sun conditions: (a) 100, (b) 50, (c) 10, (d) 5 mW/cm².

Table 2. EIS Elements of DSSC Employed with EL1–EL3 under Various Light Conditions

light intensities (mW/cm ²)	electrolyte formulation	R_{CT} (ohm-cm ²)	R_{TiO_2} (ohm-cm ²)	Z_D (ohm-cm ²)
100	EL1	2.98	4.86	2.66
	EL2	3.39	5.11	6.71
	EL3	3.95	5.48	12.02
50	EL1	2.99	7.86	2.37
	EL2	3.40	8.76	6.27
	EL3	3.94	9.40	12.65
10	EL1	3.35	37.1	2.43
	EL2	3.90	39.04	6.61
	EL3	4.52	44.68	12.89
5	EL1	3.80	68.14	2.44
	EL2	4.08	73.78	6.96
	EL3	4.66	74.68	13.22

EL3. In other words, DSSC fabricated with EL1 loses more incident light than others do and hence loses photocurrent as well. Therefore, J_{SC} of EL2 and EL3 should be higher than J_{SC} of EL1.

However, if $[I_3^-]$ is too low, it may reach mass transport limitation more easily. Figure 6 is the linear sweep voltammetry (LSV) of EL1–EL3 with Pt microelectrode. A two-step sigmoid response representing iodide oxidation and tri-iodide reduction is observed from -0.75 to 0.75 V. Here we focus on the reduction part for $I_3^- + 2e^- \rightarrow 3I^-$; the limiting current density (J_{lim}) of EL1, EL2, and EL3 is calculated to be 93.6, 33.1, and 15.1 mA/cm², respectively. It is worth emphasizing that according to previous studies,^{34,35} the bulk diffusion behavior

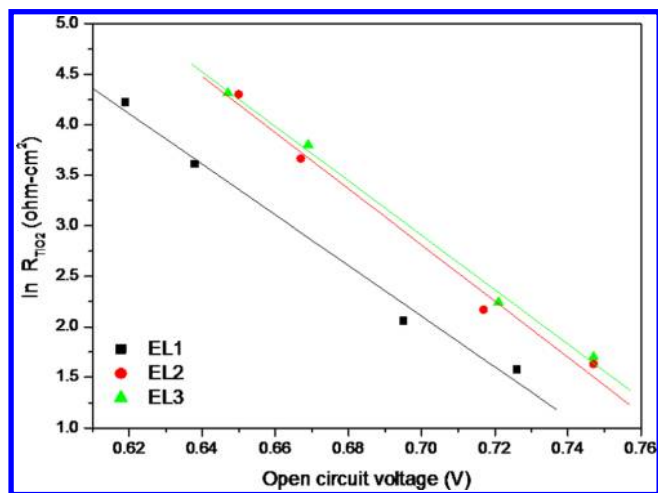


Figure 4. Dependence of R_{TiO_2} on V_{OC} for DSSCs employed with EL1–EL3.

is usually faster than that in real DSSC due to the porous structure of the dye–TiO₂ film and the factor is approximately 2.³⁴ In our system at 100 mW/cm² light intensity, J_{SC} is around 17 mA/cm², which is much smaller than one-half of the J_{lim} of EL1, meaning ion transportation between the photoanode and the counter electrode is very smooth and hence fast enough to support the J_{SC} . For the case of EL2, one-half of J_{lim} of EL2 is 16.6 mA/cm², just located in the margin of the J_{SC} level under the highest light intensity in this study; in this situation, the tri-iodide ions near the dye–TiO₂ surface are completely depleted under short-circuit conditions and the tri-iodide ions in the

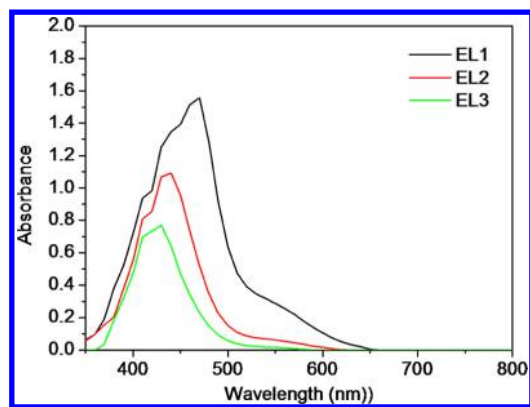


Figure 5. UV-vis spectrum of EL1–EL3 from 350 to 800 nm (1 μL of electrolyte was diluted with 60 μL of MPN).

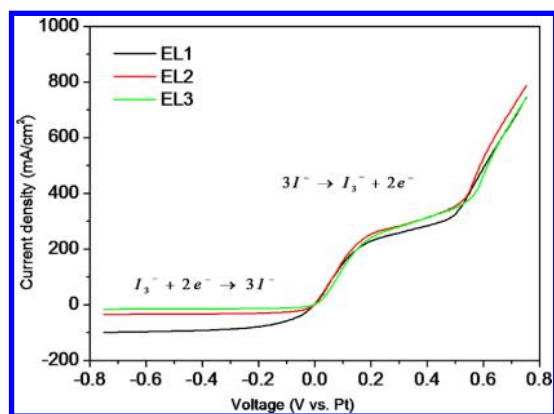


Figure 6. LSV of EL1–EL3 with Pt ultramicroelectrode (scan rate 5 mV/s).

bulk region need time to diffuse to the dye–TiO₂ surface to regenerate dye molecule. As a result, the diffusion resistance increases and FF decreases. This analysis can be further proved in the EIS discussed below.

Using Fick's law and appropriate boundary conditions, the ion diffusion impedance, Z_D , can be expressed as³²

$$Z_D = \frac{Z_0}{(i\omega)^\alpha} \tanh(i\tau_d' \omega)^\alpha \quad (4)$$

where ω is the angular frequency and α is 0.5 for a finite length Warburg impedance (FLW). Z_0 and τ_d' are the Warburg parameter and characteristic diffusion time constant, which can be represented by

$$Z_0 = \frac{RT}{n^2 F^2 [I_3^-] A \sqrt{D}} \quad (5)$$

where R is the molar gas constant, T is the temperature, F is the Faraday constant, A is the surface area of the electrode, and D is the diffusion coefficient of I_3^- .

Equation 5 implies Z_D is inversely related to $[I_3^-]$. Z_D as a function of $[I_3^-]$ under various light intensities is plotted in Figure 7. From Figure 7, it is found that Z_D of each electrolyte system is independent of light intensity but dependent on $[I_3^-]$. For instance, when $[I_3^-]$ decreases from 0.15 to 0.01875 M, Z_D increases from 2.66 to 12.02 $\text{ohm}\cdot\text{cm}^2$ at 100 mW/cm^2 illumination. The increase of Z_D contributes to the diffusion overpotential of a DSSC, and hence, FF decreases. A worst case of ion diffusion in this study happens in EL3. Due to its poor

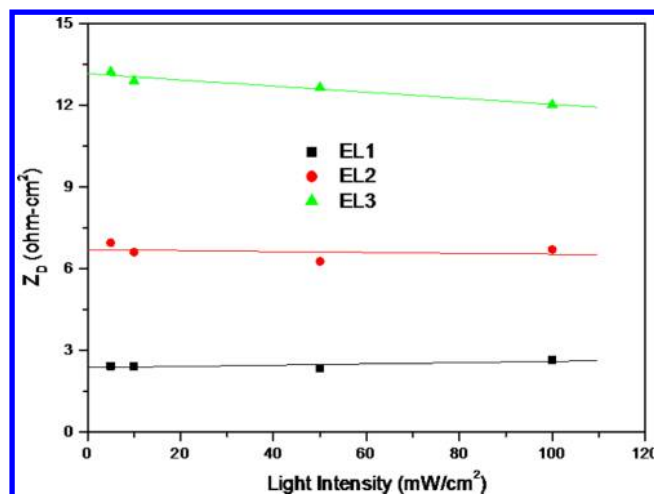


Figure 7. Z_D as a function of $[I_3^-]$ under various light intensities.

J_{lim} (15.1 mA/cm^2), it can support only up to 7 or 8 mA/cm^2 of J_{SC} before reaching the diffusion limitation.

Taking both the color effect and diffusion limitation into account, DSSC composed of EL2 shows the highest J_{SC} under 100 mW/cm^2 while DSSC composed of EL3 shows the highest J_{SC} to others under lower light intensity.

Influence of Iodine Content on the Charge Transfer Resistance, R_{CT} . Figure 8 shows the dependence of the charge

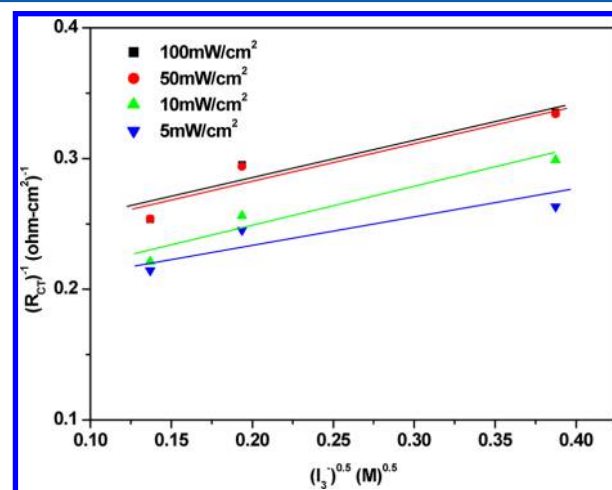


Figure 8. $1/R_{\text{CT}}$ as a function of the square root of $[I_3^-]$ under various light intensities.

transfer resistance (R_{CT}) on the concentration of tri-iodide, $[I_3^-]$. The measured data suggested a linear relationship of $1/R_{\text{CT}}$ and the square root of $[I_3^-]$, which is in a good agreement with the literature.³⁶ Though the trend is correct, the linearity is not matched perfectly, particularly in the low light illumination. This may be attributed to the PVP-entanglement interference in the vicinity of the Pt nanocluster surface when ions diffuse in and out.¹⁰ In addition, Figure 8 also reveals R_{CT} slightly increases as light intensity decreases; this may result from an instantaneous heating effect of the electrolyte at strong light.³⁷

R_{CT} is not only a key index for counter electrode performance but also an important parameter for a highly efficient DSSC. If R_{CT} is too large, this charge transfer overpotential will contribute an uncompensated voltage drop during IV measurement and result in a low FF of a DSSC.

Fortunately, the level of R_{CT} variation in our experiments is from 2.98 to 4.66 ohm-cm², meaning that the voltage drop caused by the charge transfer overpotential is a mere 10–50 mV even at short-circuit conditions. Hence, the R_{CT} variation in this study has a minor effect on cell performance.

Influence of Iodine Content on Fill Factor, FF. Fill factor (FF) indicates the deflection of the device from “resistance-free” ideal solar cells and can be taken as the overall resistance in the device or a combination of R_0 , Z_{TiO_2} , R_{CT} , and Z_D . When the DSSC is under an illumination of 100 and 50 mW/cm², the FF decreases gradually with reducing iodine content resulting from less effective ion diffusion (or the increase in ion diffusion resistance). However, at further reduced illumination intensity, the FF remains unchanged with different iodine content, which suggests either that the negative ion diffusion resistance is balanced by the positive electron recombination resistance or the iodine concentration studied in the present work is sufficiently high to provide needed charge transport through the electrolyte. In other words, the number of charges generated by incident photons is so small that the lowest iodine content would be sufficient for charge transport through the electrolyte.

Influences of Iodine Content on the Power Conversion Efficiency, PCE. Taking all of the above-mentioned factors into account, the PCE at 100 mW/cm² for EL1, EL2, and EL3 are 8.31%, 8.02%, and 7.28%, respectively. As discussed above, the gradual decrease is mainly dominated by electrolyte diffusion. On the other hand, the PCE at 50 mW/cm² is 9.79% (EL1), 10.08% (EL2), and 10.16% (EL3), which is better than that at 100 mW/cm²; this improvement originates from two positive effects of the cell including less electron recombination and less diffusion overpotential under 50 mW/cm² than 100 mW/cm²; the former factor improves V_{OC} , while the latter improves FF. Moreover, at 0.5 sun condition, the color effect becomes important as the amount of incident light is valuably limited. Under this situation, less $[I_3^-]$ is beneficial to the photoexcitation reaction since a lower fraction of incident light is adsorbed when $[I_3^-]$ is low. In other words, at low light intensity it is more effective to use an electrolyte system with higher transparency than fast ion diffusion. Therefore, at 5 mW/cm², the best performance takes place in the EL3 system, which is over 12%.

To clearly present the efficiency difference under various light illumination intensities, the relative efficiency of these three electrolyte systems is illustrated in Figure 9. Compared

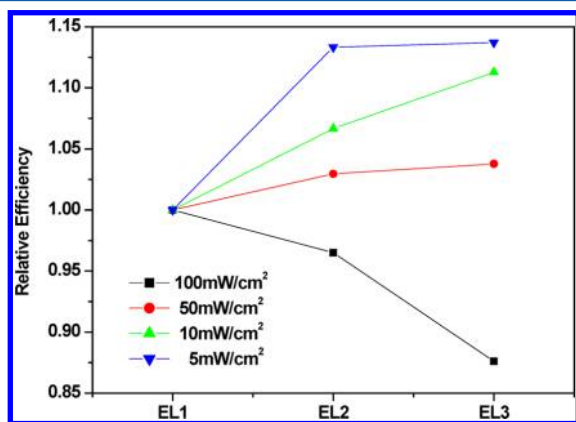


Figure 9. Relative efficiency of EL1–EL3 under various light intensities.

with the EL1 system, due to the contest of electrolyte diffusion, electron recombination, charge transfer on the cathode, and natural color of electrolyte, the EL3 system can improve nearly 14% by efficiency at 5 mW/cm², 11% at 10 mW/cm², and 4% at 50 mW/cm² but deteriorate by 13% at 100 mW/cm². This strikingly PCE improvement from 10.58% in EL1 to 12.03% in EL3 under 5mW/cm² tells us by simply optimizing the $[I_3^-]$ content in the electrolyte it is possible to optimize PCE under various illuminating environment.

4. CONCLUSIONS

The iodine content in the electrolyte has demonstrated an appreciable impact on V_{OC} , J_{SC} , and FF of DSSC under otherwise identical conditions, and such influences become more significant at lower light intensity. Combining the effects of electron recombination, electrolyte diffusion, and charge transfer reaction, lower iodine content electrolyte offers higher power conversion efficiency at lower light intensity due to there being less electron recombination taking place at the interface of TiO₂/dye/electrolyte and its light color (high transparency) can also increase the light absorption. The DSSC performance can be improved by optimizing the iodide/iodine ratio in the electrolyte to suit different DSSC applications under various operating light conditions.

■ AUTHOR INFORMATION

Corresponding Author

*E-mail: tcwei@mx.nthu.edu.tw, gzcao@u.washington.edu.

Notes

The authors declare no competing financial interest.

■ ACKNOWLEDGMENTS

The authors gratefully acknowledge the technical support from Tripod Technology Corp.

■ REFERENCES

- O'Regan, B.; Grätzel, M. *Nature* **1991**, *353*, 737–740.
- Nazeeruddin, M. K.; Kay, A.; Humphry-Baker, R.; Müller, E.; Liska, P.; Vlachopoulos, N.; Grätzel, M. *J. Am. Chem. Soc.* **1993**, *115* (14), 6382–6390.
- Grätzel, M. *Inorg. Chem.* **2005**, *44*, 6841–6851.
- Ito, S.; Matsui, H.; Okada, K.; Kusano, S.; Kitamura, T.; Wada, Y.; Yanagida, S. *Sol. Energy Mater. Sol. Cells* **2004**, *82*, 421–429.
- Yella, A.; Lee, H. W.; Tsao, H. N.; Yi, C.; Chandiran, A. K.; Nazeeruddin, M. K.; Diau, E.; Yeh, C. Y.; Zakeeruddin, S. M.; Grätzel, M. *Science* **2011**, *334*, 629–634.
- Tetreault, N.; Grätzel, M. *Energy Environ. Sci.* **2012**, *5*, 8506–8516.
- Zhang, Q.; Park, K.; Xi, J.; Myers, D.; Cao, G. *Adv. Energy Mater.* **2011**, *1*, 988–1001.
- Nazeeruddin, M. K.; Péchy, P.; Grätzel, M. *Chem. Commun.* **1997**, 1705–1706.
- Papageorgiou, N.; Maier, W. F.; Grätzel, M. *J. Electrochem. Soc.* **1997**, *144* (3), 876–884.
- Wei, T. C.; Wan, C. C.; Wang, Y. Y.; Chen, C. M.; Shiu, H. S. *J. Phys. Chem. C* **2007**, *111* (12), 4847–4853.
- Murakami, T. N.; Ito, S.; Wang, Q.; Nazeeruddin, M. K.; Bessho, T.; Cesar, I.; Liska, P.; Humphry-Baker, R.; Comte, P.; Péchy, P.; Grätzel, M. *J. Electrochem. Soc.* **2006**, *153*, A2255–A2261.
- Wolfbauer, G.; Bond, A. M.; Eklund, J. C.; MacFarlane, D. R. *Sol. Energy Mater. Sol. Cells* **2001**, *70*, 85–101.
- Kalyanasundaram, K.; Grätzel, M. *Coord. Chem. Rev.* **1998**, *177*, 347–414.
- Kern, R.; Sastrawan, R.; Ferber, J.; Stangl, R.; Luther, J. *Electrochim. Acta* **2002**, *47*, 4213–4225.

- (15) Han, L.; Koide, N.; Chiba, Y.; Mitate, T. *Appl. Phys. Lett.* **2004**, *84*, 2433–4235.
- (16) Hoshikawa, T.; Yamada, M.; Kikuchi, R.; Eguchi, K. *J. Electrochem. Soc.* **2005**, *152*, E68–73.
- (17) Bisquert, J.; Garcia-Belmonte, G.; Fabregat-Santiago, F.; Ferriols, N. S.; Bogdanoff, P.; Pereira, E. C. *J. Phys. Chem. B* **2000**, *104* (10), 2287–2298.
- (18) Wang, Q.; Ito, S.; Grätzel, M.; Fabregat-Santiago, F.; Mora-Seró, I.; Bisquert, J.; Bessho, T.; Imai, H. *J. Phys. Chem. B* **2006**, *110*, 25210–25221.
- (19) Wang, Q.; Moser, J.-E.; Grätzel, M. *J. Phys. Chem. B* **2005**, *109*, 14945–14953.
- (20) Hinsch, A.; Kroon, J. M.; Kern, R.; Uhlendorf, I.; Holzbock, J.; Meyer, A.; Ferber, J. *Prog. Photovoltaics Res. Appl.* **2001**, *9*, 425–438.
- (21) Kato, N.; Takeda, Y.; Higuchi, K.; Takeichi, A.; Sudo, E.; Tanaka, H.; Motohiro, T.; Sano, T.; Toyoda, T. *Sol. Energy Mater. Sol. Cells* **2009**, *93*, 893–897.
- (22) Koide, N.; Islam, A.; Chiba, Y.; Han, L. *J. Photochem. Photobiol., A: Chem.* **2006**, *182*, 296–305.
- (23) Wei, T. C.; Wang, Y. Y.; Wan, C. C. *Appl. Phys. Lett.* **2006**, *88*, 103122.
- (24) Lan, J. L.; Wan, C. C.; Wei, T. C.; Hsu, W. C.; Peng, C.; Chang, Y. H. *Int. J. Electrochem. Sci* **2011**, *6*, 1230–1236.
- (25) Lan, J. L.; Wan, C. C.; Wei, T. C.; Hsu, W. C.; Chang, Y. H. *Prog. Photovoltaics Res. Appl.* **2012**, *20*, 44–50.
- (26) Ito, S.; Liska, P.; Comte, P.; Charvet, R.; Péchy, P.; Bach, U.; Schmidt-Mende, L.; Zakeeruddin, S. M.; Kay, A.; Nazeeruddin, M. K.; Grätzel, M. *Chem. Commun.* **2005**, *34*, 4351–4353.
- (27) Sommeling, P. M.; O'Regan, B. C.; Haswell, R. R.; Smit, H. J. P.; Baker, N. J.; Smits, J. J. T.; Kroon, J. M.; Roosmalen, J. A. M. *J. Phys. Chem. B* **2006**, *110*, 19191–19197.
- (28) Luque, A.; Hegedus, S. *Handbook of photovoltaic science and engineering*; John Wiley and Sons, Inc.: New York, 2005.
- (29) Bisquert, J. *Phys. Chem. Chem. Phys.* **2000**, *2*, 4185–4192.
- (30) Bisquert, J. *J. Phys. Chem. B* **2002**, *106*, 325–333.
- (31) Lagemaat, J.; Park, N. G.; Frank, A. J. *J. Phys. Chem. B* **2000**, *104*, 2044–2052.
- (32) Kern, R.; Sastrawan, R.; Ferber, J.; Stangl, R.; Luther, J. *Electrochim. Acta* **2002**, *47*, 4213–4225.
- (33) Salvador, P.; Hidalgo, M. G.; Zaban, A.; Bisquert, J. *J. Phys. Chem. B* **2005**, *109*, 15915–15926.
- (34) Lindstrom, H.; Rensmo, H.; Sodergren, S.; Solbrand, A.; Lindquist, S. *J. Phys. Chem. B* **1996**, *100*, 3084–3088.
- (35) Liu, Y.; Hagfeldt, A.; Xiao, X.; Lindquist, S. *Sol. Energy Mater. Sol. Cells* **1998**, *55*, 267–281.
- (36) Hauch, A.; Georg, A. *Electrochim. Acta* **2001**, *46*, 3457–3466.
- (37) Santiago, F.; Bisquert, J.; Palomares, E.; Otero, L.; Kuang, D.; Zakeeruddin, S. M.; Graetzel, M. *J. Phys. Chem. C* **2007**, *111*, 6550–6560.